RSC Advances

PAPER

View Article Online
View Journal | View Issue

CrossMark click for updates

Cite this: *RSC Adv.*, 2017, **7**, 6006

Preparation of highly efficient antibacterial polymeric films *via* the modulation of charge density and hydrophobicity

Li-Hua Yin,†[ab] Bin Ran,[b] Tian-Jiao Hu,[b] Chen Yang,[b] Jun-Jie Fei[a] and Yi-He Li*[bc]

Received 31st October 2016
Accepted 2nd December 2016

DOI: 10.1039/c6ra26071c

www.rsc.org/advances

Highly efficient antibacterial polymeric films were prepared in a facile manner *via* a thiol–ene reaction assisted by ultraviolet radiation. The influence of the positive charge density and hydrophobicity on the antimicrobial activity was evaluated with *Escherichia coli* and *Staphylococcus aureus*. There was a synergetic enhancement in sterilization in the presence of a positive charge density and hydrophobicity, which provided a convenient way to design and synthesize highly effective antimicrobial polymers. The prepared films, with abundant cations and sufficient hydrophobicity, exhibited robust antibacterial effects against *E. coli* and *S. aureus*. Their excellent thermostability makes these films suitable for practical applications.

Open Access Article. Published on 18 January 2017. Downloaded on 8/8/2025 6:24:59 PM.
This article is licensed under a Creative Commons Attribution 3.0 Unported Licence.

Introduction

Antibiotic resistance in humans and animals is a growing public health concern worldwide,[1] especially in healthcare,[2,3] public facilities and food safety. Animals and plants both possess potent broad spectrum antimicrobial peptides (AMPs) that protect them from microbial infection.[4] The Shai–Matsuzaki–Huang model[5,6] is used to interpret the activity of AMPs (Scheme 1a). This model emphasizes the importance of electrostatic interactions between the positive AMPs and the negative bacterial membranes and hydrophobic interactions. Electrostatic interactions facilitate the association of cationic AMPs with the anionic bacterial membrane and hydrophobicity strengthens this association, which will physically disrupt the membrane structure and lead to bacterial death.

Inspired by the antimicrobial properties of AMPs, a series of polymers (Scheme 1b) designed to mimic the amphiphilic features of AMPs, including the cationic hydrophilic groups and hydrophobic moieties, have recently been reported.[7] Tiller *et al.*[8,9] prepared alkylated pyridinium polymers coated onto glass slides, which killed bacteria *via* covalent attachment. Gottenbos *et al.*[10] synthesized three methacrylate polymers and copolymers with different surface charge densities and studied their antimicrobial effects on Gram-negative and Gram-positive bacilli. The Gram-negative bacilli were inhibited by the polymers with positively charged surfaces.[11] Whitten and coworkers[12,13] reported that poly(phenylene ethynylene) with pendant quaternary ammonium groups or alkylpyridinium groups inhibited the growth of Gram-negative and Gram-positive bacteria either in solution or an immobilized phase.

Many researchers have explored the roles of charge density and hydrophobicity in antimicrobial activity;[14–17] however, there has been little research on how to control either of these two key parameters separately. We therefore synthesized a series of diallylimidazolium-based polymers with different ratios of hydrophobicity and charge density *via* the facile thiol–ene click reaction; thiol–ene photochemistry provides a convenient single-step approach to the synthesis of cross-linked polymers.[18–22] The characteristics of the polymerization reaction, such as a step-growth mechanism[23] and mild reaction conditions,[24] low temperatures, rapid polymerization[25] and oxygen-resistance are suitable for many biomolecular purposes.[26] We introduced an antibacterial agent 1-allyl-3-decylimidazolium bromide (ADIm)[20] and used *N*,*N*-diallylimidazolium (DIm) bromide as the cross-linking agent. Both of these species provide double bonds and cations and the alkyl chains provided by ADIm act as hydrophobic groups. By carefully balancing the two factors, optimum sterilization was obtained.

Experimental section

Materials

Unless otherwise stated, all materials were obtained from commercial suppliers without further purification. Acetonitrile, ethanol, ethyl acetate, petroleum ether, sodium hydroxide and imidazole were of analytical-reagent grade and were obtained from Sinopharm Chemical Reagent Co. 1-Bromodecane (>98%) was purchased from Aladdin. Allyl bromide (>98%), 1-allylimidazole (98%), 2,4,6-triallyloxy-1,3,5-triazine (TAC, 99%) and 2,2-dimetho-xy-2-phenylacetophenone (DMPA, 98%) were obtained

[a]College of Chemistry, Xiangtan University, Xiangtan 411100, China
[b]College of Science, National University of Defense Technology, Changsha 410073, China. E-mail: yhli@nudt.edu.cn
[c]State Key Library of NBC Protection for Civilian, Beijing 102205, China
† Worked at Prof. Yi-He Li's lab under a co-advisor program.

This journal is © The Royal Society of Chemistry 2017

Open Access Article. Published on 18 January 2017. Downloaded on 8/8/2025 6:24:59 PM.
This article is licensed under a Creative Commons Attribution 3.0 Unported Licence.

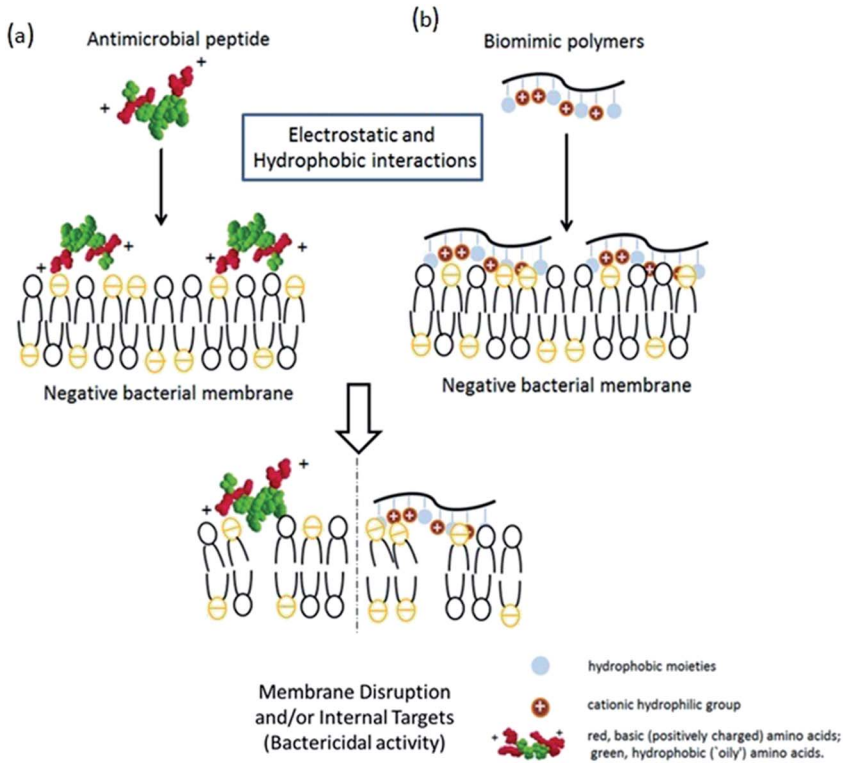

Scheme 1 Antimicrobial effects *in vivo* and *in vitro*.

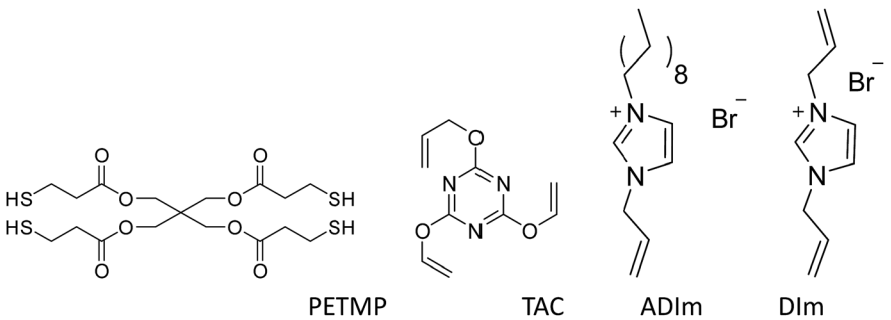

Scheme 2 Structures of investigated compounds.

from J&K. Pentaerythritol tetra(3-mercaptopropionate) (PETMP, 90%) was purchased from Micxy Reagent. The main compounds investigated in the study are shown in Scheme 2.

Synthesis of *N*,*N*-diallylimidazolium bromide

1-Allylimidazole (7 ml, 64 mmol), allyl bromide (5.54 ml, 64 mmol) and 20 ml of ethanol were added to a 100 ml flask under a nitrogen atmosphere. The reaction mixture was refluxed for 20 h. After removing the solvent, the residue was washed three times with hexane. This compound was obtained as a dark green viscous oil at a yield of 90%. ^{1}H NMR (400 MHz; DMSO): δ 9.24 (1H, s, N–CH–N), 7.76 (2H, s, CH in imidazolium ring), 5.98–6.08 (2H, m, –CH=CH_2), 5.25–5.35 (4H, m, CH_2=CH–), 4.85–4.86 (4H, d, N–CH_2–) ppm.

Synthesis of antibacterial polymer films with a charge density gradient and films with variable hydrophobicity

The general procedure for the synthesis of antibacterial polymer films with a charge density gradient (film-CDG) was as follows. The UV-curable formulation was prepared by mixing PETMP, a compound cross-linking agent consisting of TAC and/or DIm, with ADIm in five serum bottles using a magnetic stirrer. The composition of all formulations is given in Table 1. After stirring to obtain a homogeneous mixture, DMPA (48 mg, 0.187 mmol) dissolved in DMF (50 μL) was added to the bottle as a photoinitiator and the mixture was stirred for 10 s. The formulations were then coated on a round glass pane (22 × 22 mm) using a film applicator and irradiated on a an Exposure Model RW-UVAT201-20 UV-curing conveyor system (RunWing

Open Access Article. Published on 18 January 2017. Downloaded on 8/8/2025 6:24:59 PM.
This article is licensed under a Creative Commons Attribution 3.0 Unported Licence.

Table 1 Compositions of the antibacterial polymer films with a variable charge density

Entry	Symbol	$n_T : n_D$	TAC (mg)	DIm (mg)	ADIm (mg)	PETMP (mg)
1	Film-CDG1	1 : 0	272	0	135	500
2	Film-CDG2	2 : 1	204	241	135	500
3	Film-CDG3	1 : 1	163	169	135	500
4	Film-CDG4	1 : 2	117	241	135	500
5	Film-CDG5	0 : 1	0	422	135	500

Table 2 Compositions of the antibacterial polymer films with variable hydrophobicity with variable ADIm contents

Entry	Symbol	ADIm (mg)	TAC (mg)	DIm (mg)	PTEMP (mg)
1	Film-VH1	0 (0%)	0	468	500
2	Film-VH2	135 (10%)	31	374	500
3	Film-VH3	337 (25%)	75	234	500
4	Film-VH4	673 (50%)	151	0	500

Co. Ltd, Shenzhen, China) equipped with a 2 kW Hg lamp at a conveyor speed of 3 m min^{-1} for 20 s exposure in one run.

The general procedure for the synthesis of antibacterial polymer films with variable hydrophobicity (film-VH) was as follows. The procedure for the film-VH was similar to that described previously. The ADIm content was increased systematically to obtain a series of different alkyl chain lengths. The amount of TAC and DIm were adjusted and controlled to maintain the amount of total cations in ADIm and DIm. The composition of all formulations is given in Table 2.

Characterization

X-ray photoelectron spectroscopy (XPS) was performed using an S-probe spectrometer (Surface Science Instruments, Mountain View, CA, USA) with monochromatic X-rays (10 kV, 22 mA, spot size 250 × 1000 μm) sourced from an aluminum anode to monitor the composition of the film-CDG. The attenuated total reflection Fourier transform infrared (ATR-FTIR) spectra were recorded on a Thermo Nicolet IR spectrometer. The isosorbide-derived films (6–8 mg) were introduced into aluminum pans and were analyzed using a PerkinElmer Diamond DSC instrument under a nitrogen atmosphere. The samples were first scanned from −80 to 100 °C at a heating rate of 10 °C min^{-1} and then cooled to −80 °C at 100 °C min^{-1}, and finally heated again to 80 °C at a heating rate of 100 °C min^{-1}. The second heating run was used to determine the glass transition temperature (T_g). Thermogravimetric analysis (TGA) was performed with a Mettler TGA/DSC instrument between 25 and 500 °C at a heating rate of 10 °C min^{-1} under a flow nitrogen.

Assessment of antibacterial activity

Gram-negative *Escherichia coli* (ATCC 25922) and Gram-positive *Staphylococcus aureus* (ATCC 29213), species commonly related to infections associated with biomaterials, were used to evaluate the antibacterial efficacy of the polymer films. After the frozen *E. coli* and *S. aureus* stock had been defrosted, they were cultured overnight in an incubator at 37 °C on Luria–Bertani and Manitol Salt agar plates, respectively. A single colony was incubated for 12 h at 37 °C in 5 ml of Nutrient Bertani broth to grow statically for activation. After incubation, the bacterial suspension was centrifuged and the supernatant was decanted. The bacterial cells were resuspended and washed twice with PBS and then resuspended in 10 ml of PBS at 6×10^7 cells per ml. Each film was then immersed in the bacterial suspension at 37 °C by shaking in an orbital incubator to ensure a good contact between the antimicrobial films and the bacteria. The viability of the bacteria on the polymer films was quantified using the spread plate method by sampling an equal amount of the bacterial suspension at 20, 40 and 60 min.

Results and discussion

N,*N*-1-Allyl-3-decylimidazolium (ADIm)-based polymers have previously been reported to have a good antibacterial effect on both Gram-negative and Gram-positive bacteria containing long alkyl chains.[20,27] ADIm was therefore chosen as the hydrophobic component in this work and the charge density was modulated by changing the ratio of *N*,*N*-diallylimidazolium bromide (DIm) and ADIm. By varying the amount of ADIm, DIm and the thiol cross-linking agent, the hydrophobicity and charge density could be accurately controlled (Scheme 3).

We studied the effect of the charge density on the antibacterial activity. An identical amount of ADIm was used in each polymer to maintain the hydrophobicity at the same level. Table 1 shows that the charge density was gradually changed by varying the ratio of TAC and DIm. XPS was used to determine the charge difference in five samples (Fig. 1). The N 1s core-level spectrum could be curve-fitted into two peak components. The peak component at a binding energy (BE) of 399.7 eV was attributable to the amine (C)═N group in TAC.[10] The peak component at a BE of 401.5 eV was associated with the positively charged nitrogen (–N^+–) in DIm and ADIm.[28] As expected, the positively charged nitrogen (–N^+–) peak component in the N 1s core-level spectra became stronger as the amount of DIm increased, reflecting the increase in charge density on the polymer films.

We evaluated the antibacterial activity of the film-CDGs using *E. coli* and *S. aureus* (Fig. 2). The as-prepared films showed antibacterial activity at a contact time of 60 min and the activity improved as the density of the positive charge increased. For *E. coli*, when the ratio of *T* to *D* was ≥1 : 1, the corresponding film (film-CDG3-5) killed them all in <40 min. Similar results were obtained for *S. aureus*. *S. aureus* was more sensitive to the density of positive charge than *E. coli*. *S. aureus* was quantitatively killed in <40 min when the ratio of *T* to *D* was 2 : 1. At a ratio of 0 : 1, *S. aureus* was killed very quickly, indicating a very high efficiency. The film with this composition (entry 5 in Table 1) could be used as a prototype for further optimization. The observed positive correlation between the antibacterial activity and the density of the positive charges indicated the importance of the effect of electrostatic absorption on the antibacterial activity.

 This journal is © The Royal Society of Chemistry 2017

Open Access Article. Published on 18 January 2017. Downloaded on 8/8/2025 6:24:59 PM.
This article is licensed under a Creative Commons Attribution 3.0 Unported Licence.

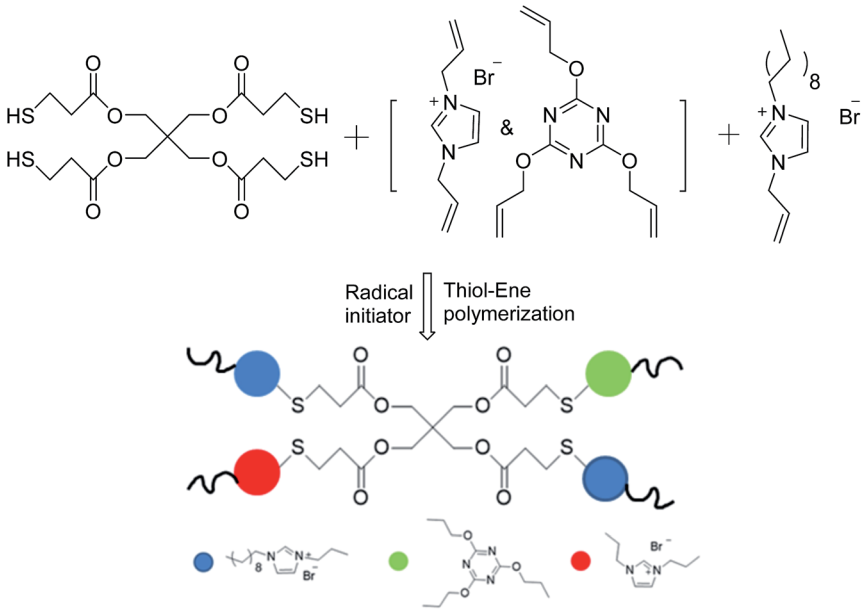

Scheme 3 Chemical representation of the antimicrobial film.

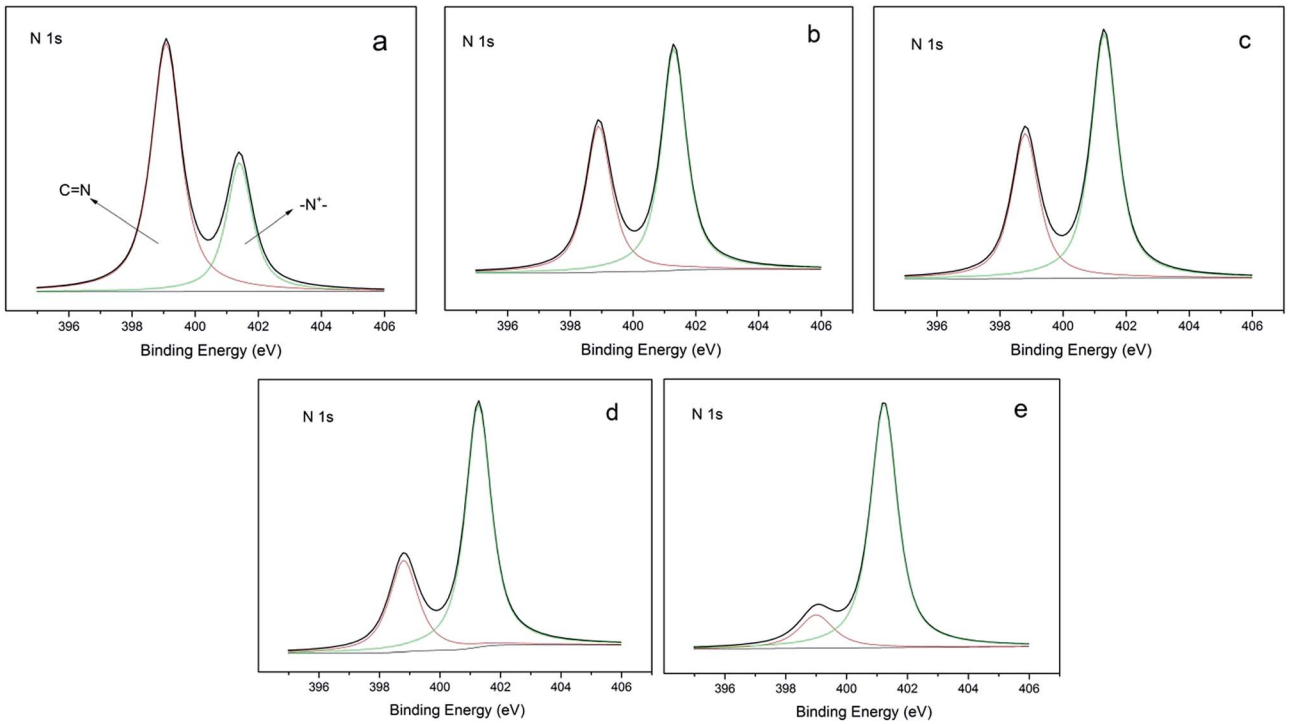

Fig. 1 XPS N 1s core-level spectra of the film-CDG: (a) $n_T : n_D = 1 : 0$; (b) $n_T : n_D = 2 : 1$; (c) $n_T : n_D = 1 : 1$; (d) $n_T : n_D = 1 : 2$; and (e) $n_T : n_D = 0 : 1$ surface.

The thermal stability of the antimicrobial films was studied by thermal gravimetric analysis (TGA) under a nitrogen atmosphere at a heating rate of 10 °C min^{-1} (Fig. 3). All the films showed good thermostability at <200 °C without any obvious decomposition. The thermostability was further enhanced by the increased charge density. For example, the thermostability of film-CDG4 reached 300 °C. The good thermal performance of these films may be applicable in harsh environments.

Relationship between antibacterial activity of polymer films and hydrophobicity

Having confirmed the effect of the positive charge on sterilization, we investigated the effect of hydrophobicity on antibacterial activity. Four films with different amounts of alkyl chains (*i.e.* variable hydrophobicity) were prepared. The ADIm content was increased systematically to obtain polymers with different

Open Access Article. Published on 18 January 2017. Downloaded on 8/8/2025 6:24:59 PM.
This article is licensed under a Creative Commons Attribution 3.0 Unported Licence.

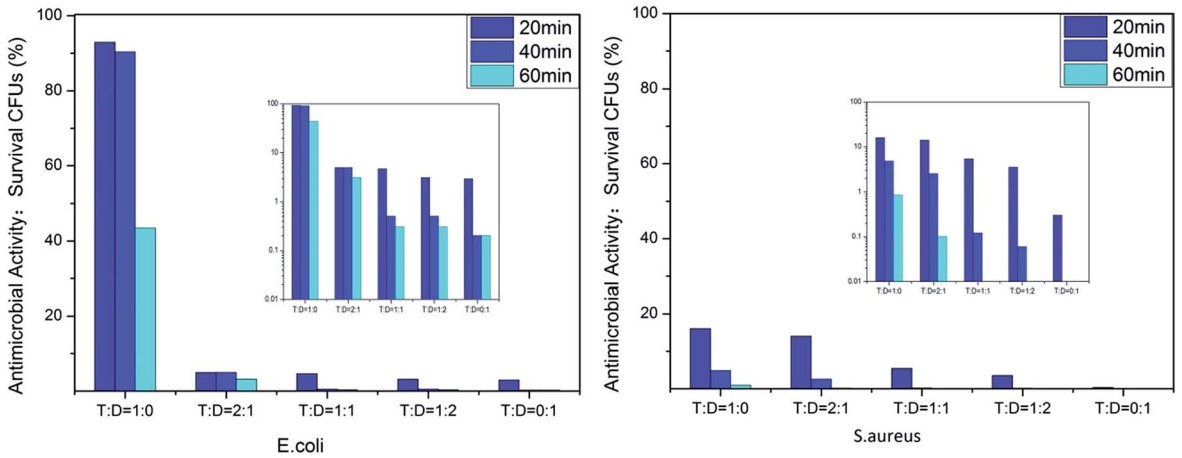

Fig. 2 Antibacterial activity of films-CDG against *E. coli* and *S. aureus*.

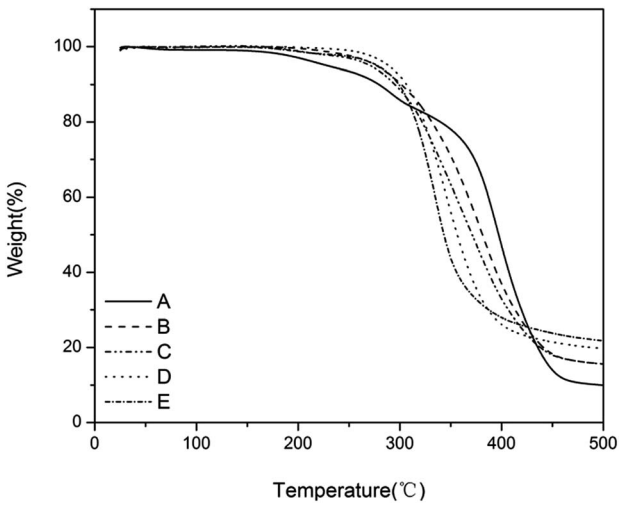

Fig. 3 TGA curve of the films with a charge density gradient. (A) $T : D = 1 : 0$, (B) $T : D = 2 : 1$, (C) $T : D = 1 : 1$, (D) $T : D = 1 : 2$ and (E) $T : D = 0 : 1$.

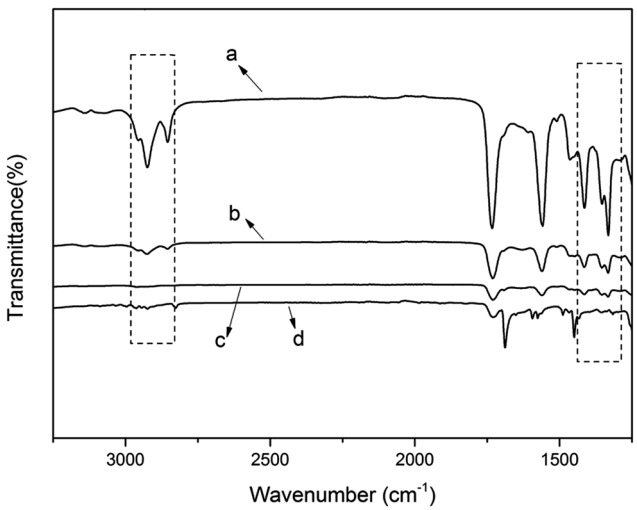

Fig. 4 ATR-FTIR spectra of the film-VH (a) contained 50% ADIm, (b) contained 25% ADIm, (c) contained 10% ADIm, and (d) contained 0% ADIm.

hydrophobicity. The amounts of TAC and DIm were adjusted to maintain a constant value for the total cations. The compositions of examined polymers (film-VH) are given in Table 2.

The hydrophobic groups (*e.g.* methyl and methylene) were monitored using ATR-FTIR (Fig. 4). The peaks at 2960, 2850, 1460 and 1380 cm^{-1} represent the absorption of methyl and methylene from ADIm. As the content of the antimicrobial monomer increased, the intensity of these peaks became stronger (from d to a in Fig. 4). There was no absorption peak at 2547 cm^{-1}, indicating that most of the thiol groups had reacted. Therefore the desired films had been successfully prepared.

The antibacterial activity of the film-VHs was evaluated using *E. coli* and *S. aureus* (Fig. 5). As there was an identical amount of cations in these four samples, the influence of the hydrophobic groups on sterilization could be compared. All the films showed very good antibacterial results; however, the film without long chain alkyl groups (film-VH1) needed a longer time (40 min) to give a good antimicrobial effect than the other films. When the amount of ADIm increased from 0 to 50%, the colony-forming units (CFUs) for *E. coli* decreased from 30 to 10% after 20 min, which confirmed the role of hydrophobicity. By further extending the contact time to 40 min, *E. coli* was completely killed by film-VH1-4. These four films showed excellent antimicrobial activity against *S. aureus* within 20 min (film-VH2-4), whereas film-VH1 required more time to reach the same level of antimicrobial activity, reflecting the importance of hydrophobicity. The effect of the alkyl chain length on the antibacterial activity of the cationic antimicrobial films was complicated and was different against Gram-positive and Gram-negative bacteria. This may be because the change in the antimicrobial agent (with long alkyl chains) changes both the hydrophobicity and other factors,[29] thus influencing the antibacterial activity.

Fig. 6 shows that the thermostability of the film-VHs was similar to that of the film-CDGs. They decomposed up to 300 °C, which is in accordance with previously reported thiol–ene

 This journal is © The Royal Society of Chemistry 2017

Open Access Article. Published on 18 January 2017. Downloaded on 8/8/2025 6:24:59 PM.
This article is licensed under a Creative Commons Attribution 3.0 Unported Licence.

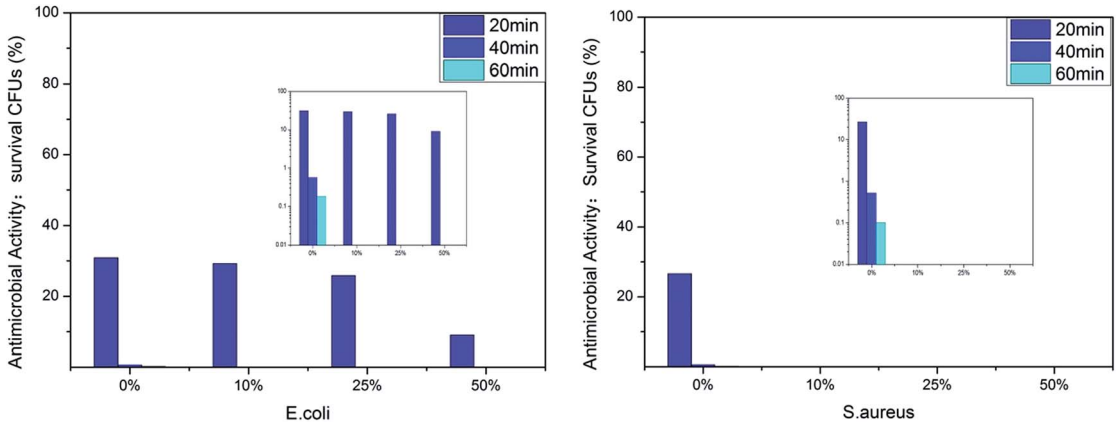

Fig. 5 Antibacterial activity of films-VH against *E. coli* and *S. aureus*.

photopolymerizable systems.[25,30] The introduction of more ADIm with long alkyl chains slightly reduced the thermostability (film-VH2-4) as the result of a reduced degree of cross-linking.

The glass transition temperature (T_g) was studied by DSC at a heating rate of 10 °C min^{-1} under a nitrogen atmosphere. The T_g values decreased with increasing amounts of DIm. This effect was more pronounced when the rigid monomer TAC was used as the alkene component; using the flexible monomer DIm as the alkene component decreased T_g for all thiol formulations. The highest T_g values were observed in the thiol–ene networks with the highest cross-linking density ($T:D = 1:0$), as expected. Replacing the trifunctional ene (TAC) with a difunctional ene (DIm) reduced T_g in concert with the average cross-linking density. T_g spanned a narrow range of temperatures. This was expected and was attributable to the monomers chosen in this investigation. Most T_g values were sub-zero or relatively low, which is typical of thiol–ene networks[31] because of the flexible thioether linkages throughout the network. Therefore the T_g values of these polymers are affected by these two opposite key factors: the flexibility of the network backbone and the cross-linking density.

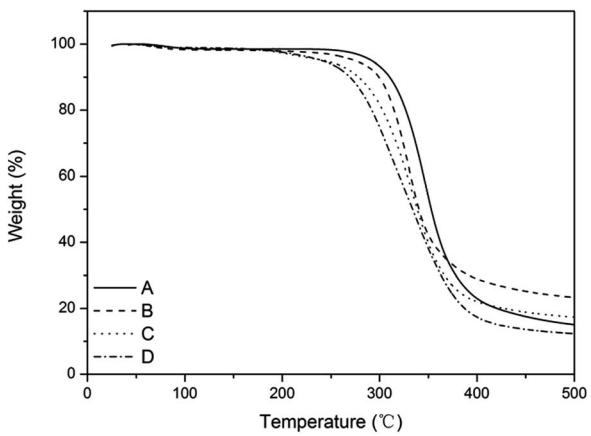

Fig. 6 TGA curve of films with variable content of alkyl chain. (A) Content of ADIm is 0, (B) content of ADIm is 10%, (C) content of ADIm is 25%, and (D) content of ADIm is 50%.

Conclusions

By varying the ratio of hydrophobicity and the charge density group, a series of polymeric films was successfully prepared *via* thiol–ene photopolymerization. This outcome of this convenient and concise assay was in good agreement with the XPS and ATR-FTIR analyses. The resulting films with abundant cations displayed a remarkable antimicrobial activity against both *S. aureus* and *E. coli*, which correlated with the electrostatic properties. The antimicrobial activity of the polymer films was positively correlated with the charge density and nature of the long alkyl chain. The polymeric antibacterial films had excellent stability under physiological conditions. The thermal stability was enhanced as the charge density increased. This method of synthesizing antibacterial polymeric films with a tunable charge density or hydrophobicity by introducing a cationic cross-linking agent is important in studies of the mechanisms involved in cationic antibacterial polymers and clarifies the effects of charge density and hydrophobicity.

References

1 M. S. Niederman and D. E. Craven, *Am. J. Respir. Crit. Care Med.*, 2005, **171**, 388–416.
2 A. B. Haynes, T. G. Weiser, W. R. Berry, *et al.*, *N. Engl. J. Med.*, 2009, **360**, 491–499.
3 T. H. Dellit, R. C. Owens, J. E. McGowan, D. N. Gerding, R. A. Weinstein, J. P. Burke, W. C. Huskins, D. L. Paterson, N. O. Fishman, C. F. Carpenter, P. J. Brennan, M. Billeter and T. M. Hooton, *Clin. Infect. Dis.*, 2007, **44**, 263–264.
4 M. Zasloff, *Nature*, 2002, **415**, 389–395.
5 K. Matsuzaki, *Biochim. Biophys. Acta*, 1999, **1462**, 1–10.
6 L. Yang, T. M. Weiss, R. I. Lehrer and H. W. Huang, *Biophys. J.*, 2000, **79**, 2002–2009.
7 L. Liu, Y. Huang, S. N. Riduan, S. Gao, Y. Yang, W. Fan, *et al.*, *Biomaterials*, 2012, **33**, 8625–8631.

Open Access Article. Published on 18 January 2017. Downloaded on 8/8/2025 6:24:59 PM.
This article is licensed under a Creative Commons Attribution 3.0 Unported Licence.

8 J. C. Tiller, C. J. Liao, K. Lewis and A. M. Klibanov, *Proc. Natl. Acad. Sci. U. S. A.*, 2001, **98**, 5981–5985.
9 J. C. Tiller, S. B. Lee, K. Lewis and A. M. Klibanov, *Biotechnol. Bioeng.*, 2002, **79**, 465–471.
10 B. Gottenbos, D. W. Grijpma, H. C. van der Mei, J. Feijen and H. J. Busscher, *J. Antimicrob. Chemother.*, 2001, **48**, 7–13.
11 B. Gottenbos, H. C. van der Mei, F. Klatter, D. W. Grijpma, J. Feijen, P. Nieuwenhuis and H. J. Busscher, *Biomaterials*, 2003, **24**, 2707–2710.
12 S. Chemburu, T. S. Corbitt, L. K. Ista, E. Ji, J. Fulghum, G. P. Lopez, K. Ogawa, K. S. Schanze and D. G. Whitten, *Langmuir*, 2008, **24**, 11053–11062.
13 T. S. Corbitt, J. R. Sommer, S. Chemburu, K. Ogawa, L. K. Ista, G. P. Lopez, D. G. Whitten and K. S. Schanze, *ACS Appl. Mater. Interfaces*, 2009, **1**, 48–52.
14 J. Ranke, M. U. Bottin-Weber, F. Stock, S. Stolte, J. Arning, R. Stoermann, *et al.*, *Ecotoxicol. Environ. Saf.*, 2007, **67**, 430–438.
15 J. Łuczak, C. Jungnickel, I. Łącka, S. Stolte and J. Hupka, *Green Chem.*, 2010, **12**, 593–601.
16 R. T. W. Huang, K. C. Peng, H. N. Shih, G. H. Lin, T. F. Chang, S. J. Hsu, *et al.*, *Soft Matter*, 2011, **7**, 8392–8400.
17 P. Zou, D. Laird, E. K. Riga, Z. Deng, F. Dorner, H. R. Perez-Hernandez, *et al.*, *J. Mater. Chem. B*, 2015, **3**, 6224–6238.
18 W. J. Yang, T. Cai, K. G. Neoh, E. T. Kang, S. L. Teo and D. Rittschof, *Biomacromolecules*, 2013, **14**, 2041–2051.
19 R. T. C. Cleophas, M. Riool, H. C. Q. V. Ufford, S. A. J. Zaat, J. A. W. Kruijtzer and R. M. J. Liskamp, *ACS Macro Lett.*, 2014, **3**, 477–480.
20 C. Zhou, Y. H. Li, Z. H. Jiang, K. D. Ahn, T. J. Hu, Q. H. Wang, *et al.*, *Chin. Chem. Lett.*, 2016, **27**, 685–688.
21 C. Zhou, Y. H. Li, Z. H. Jiang, K. D. Ahn, T. J. Hu, Q. H. Wang, *et al.*, *Chin. Chem. Lett.*, 2016, **27**, 681–684.
22 R. T. Cleophas, J. Sjollema, H. J. Busscher, J. A. Kruijtzer and R. M. Liskamp, *Biomacromolecules*, 2014, **15**, 3390–3395.
23 N. B. Cramer, T. Davies, A. K. O'Brien and C. N. Bowman, *Macromolecules*, 2003, **36**, 4631–4636.
24 B. J. Sparks, T. J. Kuchera, M. J. Jungman, A. D. Richardson, D. A. Savin, S. Hait, *et al.*, *J. Mater. Chem.*, 2012, **22**, 3817–3824.
25 B. J. Sparks, E. F. T. Hoff, L. T. P. Hayes and D. L. Patton, *Chem. Mater.*, 2012, **24**, 3633–3642.
26 K. L. Poetz, H. S. Mohammed, B. L. Snyder, G. Liddil, D. S. Samways and D. A. Shipp, *Biomacromolecules*, 2014, **15**, 2573–2582.
27 M. Kim, C. Song, K. H. Dong, K. D. Ahn, S. S. Hwang, J. A. Dong, *et al.*, *React. Funct. Polym.*, 2015, **87**, 53–60.
28 W. J. Yang, K. G. Neoh, E. T. Kang, L. M. Teo and D. Rittschof, *Polym. Chem.*, 2013, **4**, 3105–3115.
29 L. Pérez, A. Pinazo, M. T. García and M. R. Infante, *New J. Chem.*, 2004, **28**, 1326–1334.
30 L. Xue, D. Wang, Z. Yang, Y. Liang, J. Zhang and S. Feng, *Eur. Polym. J.*, 2013, **49**, 1050–1056.
31 L. Kwisnek, S. Nazarenko and C. E. Hoyle, *Macromolecules*, 2009, **42**, 7031–7041.

This journal is © The Royal Society of Chemistry 2017